Available online at www.sciencedirect.com
ScienceDirect
International Journal of Thermal Sciences 47 (2008) 507–513
International Journal of Thermal Sciences
www.elsevier.com/locate/ijts

Thermal propagation analysis for living tissue with surface heating

Kuo-Chi Liu *

Department of Mechanical Engineering, Far East University, 49 Chung Hua Rd., Hsin-Shih, Tainan, Taiwan 744

Received 3 November 2006; received in revised form 6 April 2007; accepted 10 April 2007

Available online 19 June 2007

Abstract

This work theoretically investigates the thermal behavior in a living tissue subjected to constant, sinusoidal, or step surface heatings with the thermal wave model of bioheat transfer. The attention is paid on the cases that heat mainly propagates in the direction perpendicular to the skin surface. The effects of thermal physical properties on the wave like behavior of bioheat transfer are investigated. A modified discretization scheme based on the Laplace transform is proposed to solve the present problem. The comparison between the present numerical results and those in the literature is made to evidence the present results rational and reliable.

Keywords: Bioheat transfer; Modified discretization scheme; Thermal wave model

1. Introduction

Knowledge on heat transfer in living tissues has been widely used in therapeutic applications. For further studying thermal behavior in biological bodies, many models describing bioheat transfer have been developed [1]. Due to simplicity and validity, the Pennes model is the most commonly used one among them. The applications of this relatively simple bioheat equation include simulations of hyperthermia [2–4] and cryosurgery [5,6], thermal diagnostics [7], thermal comfort analysis [8], thermal parameter estimation [9–12], and burn injury evaluation [13–19]. The Pennes bioheat equation describes the thermal behavior based on the classical Fourier's law. As is well known, Fourier's law depicts an infinitely fast propagation of thermal signal, obviously incompatible with physical reality. Thus a modified flux model for the transfer processes with a finite speed wave is suggested [20–24] and solve the paradox occurred in the classical model. This thermal wave theory introduces a relaxation time that is required for a heat flux vector to respond to the thermal disturbance (that is, temperature gradient) as

$$\vec{q} + \tau \frac{\partial \vec{q}}{\partial t} = -K \nabla T \tag{1}$$

The relaxation time is approximated as $\tau = \alpha / V^2$. Here, K is the conductivity, t time, α the thermal diffusivity, and V denotes the heat propagation velocity in the medium. The literatures [20–24] state that heating processes are shorter than the relaxation time of heat transfer medium, and the wave like behavior of heat transfer becomes the dominant form.

In homogenous materials such as common metals, the relaxation time ranges from 10^{-8} to 10^{-14} s [25–27]. The heating processes are mostly much longer than this time scale. This is why the phenomenon of the heat wave is difficult to observe in homogenous substances. In reality, the living tissues are highly nonhomogenous, and accumulating enough energy to transfer to the nearest element would take time. The literatures [25–27] and many others reported the value of τ in biological bodies to be 20–30 s. Mitra et al. [28] found the relaxation time for processed meat is of the order of 15 s. It reconfirms the order of magnitude of the values obtained by Kaminski [26]. Recently, Roetzel et al. [29] experimentally investigated the relaxation thermal behavior in nonhomogenous materials for solving the controversy proposed by Graßmann and Peters [30] and Herwing and Beckers [31], which in materials with nonhomogenous inner structure no evidence of relaxation thermal behavior exists, and obtained the value of τ about 2 s for processed meat. Yang [32] also discussed thermal shock phenomenon from biothermomechanical viewpoint. It is obvious that the wave like behavior of bioheat transfer obtains support from the literatures.

* Fax: +886 6 597 7510.
E-mail address: kcliu@cc.feu.edu.tw.

1290-0729/$ – see front matter
doi:10.1016/j.ijthermalsci.2007.04.005

Nomenclature

B	coefficient	V	heat propagation velocity in tissue ..... m/s
C	specific heat of tissue ..... J/kg °C	W_b	perfusion rate of blood ..... kg/m^3 s
C_b	specific heat of blood ..... J/kg °C	x	space coordinate ..... m
K	thermal conductivity ..... W/m °C	*Greek symbols*	
L	length of tissue ..... m	α	thermal diffusivity ..... m^2/s
ℓ	distance between two neighboring nodes ..... m	θ	elevation temperature defined as $\theta = T - T_i$ .. °C
m	node number at the boundary surface	θ_0	initial elevation temperature ..... °C
q_m	metabolic heat generation ..... J/m^3	λ	parameter defined in Eq. (10)
q_r	heat source for spatial heating ..... J/m^3	$\tilde{\theta}$	Laplace transform of θ
q_w	amplitude of sinusoidal surface heating .... J/m^3	ρ	density ..... kg/m^3
s	Laplace transform parameter	τ	relaxation time ..... s
t	time ..... s	*Subscripts*	
T	temperature of tissue ..... °C	i	node number
T_b	arterial temperature ..... °C	j	number of sub-space domain
T_i	initial temperature of tissue ..... °C		
$u(t)$	step function		

The heating actions in living tissues such as burn injury, freeze injury, scald medicine, and laser radiation are rapid. As a result, Liu et al. [33] introduced the thermal wave model of bioheat transfer for the investigation of physical mechanisms and the behaviors in thermal wave propagation in living tissues.

As Lu et al. [34] stated, the fundamental solution of the thermal wave model of bioheat transfer is very difficult to obtain. The papers studying the relevant bioheat transfer problems are still rare. The Laplace transform technique and a modified discretization scheme are proposed to solve the present problem. The effects of thermal physical properties on the wave like behavior of bioheat transfer in living tissues are investigated. To evidence the efficiency of the present numerical scheme, the comparison between the present numerical results and those in the literature [33] for the case of constant surface temperature heating is made.

2. Mathematical formulation

Energy conservation equation of bioheat transfer described in the Pennes model is

$$-\nabla\cdot\vec{q} + W_b C_b(T_b - T) + q_m + q_r = \rho C\frac{\partial T}{\partial t} \tag{2}$$

Here, ρ, C, and T denote density, specific heat, and temperature of tissue. C_b and W_b are, respectively, the specific heat and perfusion rate of blood. q_m is the metabolic heat generation and q_r is the heat source for spatial heating. T_b is the arterial temperature and was regarded as a constant.

To take account the finite heat propagation effects for more realistic predictions than that from traditional bioheat equation, Liu et al. [33] derived the thermal wave model of bioheat transfer from Eqs. (1) and (2) as

$$\begin{aligned}&\nabla\cdot(K\nabla T) + W_b C_b(T_b - T) + q_m + q_r \\ &\quad + \tau\left(-W_b C_b\frac{\partial T}{\partial t} + \frac{\partial q_m}{\partial t} + \frac{\partial q_r}{\partial t}\right) \\ &= \rho C\left(\tau\partial^2 T/\partial t^2 + \partial T/\partial t\right)\end{aligned} \tag{3}$$

It is observed that Eq. (3) is the hyperbolic heat transfer equation and is more mathematically complex than the Pennes model. As $\tau = 0$, Eq. (3) undergoes to the Pennes' bioheat equation.

This paper pay attention on the cases that heat mainly propagates in the direction perpendicular to the skin surface. As a result, one-dimensional heat transfer can be a good approximation. The 1-D form of Eq. (3) with constant thermal parameters, $q_m = \text{constant}$, and $q_r = 0$ is written as

$$\begin{aligned}&K\frac{\partial^2 T}{\partial x^2} + W_b C_b(T_b - T) + q_m - \tau W_b C_b\frac{\partial T}{\partial t} \\ &\quad = \rho C\left(\tau\partial^2 T/\partial t^2 + \partial T/\partial t\right)\end{aligned} \tag{4}$$

And then, the initial steady temperature distribution $T_i(x, 0)$ in tissue can be written from Eq. (4) as

$$K\frac{\partial^2 T_i}{\partial x^2} + W_b C_b(T_b - T_i) + q_m = 0 \tag{5}$$

Subtracting Eq. (5) from Eq. (4) leads to

$$\rho C\tau\frac{\partial^2\theta}{\partial t^2} + (\rho C + \tau W_b C_b)\frac{\partial\theta}{\partial t} + W_b C_b\theta - K\frac{\partial^2\theta}{\partial x^2} = 0 \tag{6}$$

where the elevation temperature θ is defined as $\theta = T - T_i$.

The initial conditions are to be consistent throughout this study as

$$\theta(x, 0) = 0 \quad \text{and} \quad \frac{\partial\theta(x, 0)}{\partial t} = 0 \tag{7}$$

Various types of boundary conditions will be discussed in the following illustrations.

3. Numerical analysis

The Laplace transform method is employed to map Eq. (6) into steady one. The Laplace transform of a function $\phi(t)$ with

respect to t is defined as follows:

$$\tilde{\phi}(s) = \int_0^\infty \phi(t) \mathrm{e}^{-st}\, \mathrm{d}t \tag{8}$$

where s is the Laplace transform parameter. Eq. (6) can be written in the transform domain as

$$\frac{\mathrm{d}^2\tilde{\theta}}{\mathrm{d}x^2} - \lambda^2\tilde{\theta} = 0 \tag{9}$$

where

$$\lambda^2 = \frac{1}{K}\left[\tau\rho C s^2 + (\rho C + \tau W_b C_b)s + W_b C_b\right] \tag{10}$$

The present work divides the whole space domain into several sub-space domains, as shown in Fig. 1. Thus, Eq. (10) in the jth sub-space domain can be written as

$$\frac{\mathrm{d}^2\tilde{\theta}_j}{\mathrm{d}x^2} - \lambda^2\tilde{\theta}_j = 0 \quad \text{for } x_i \leqslant x \leqslant x_{i+1},\ j = i \tag{11}$$

Eq. (11) subjected to the boundary conditions

$$\tilde{\theta}_j(x_i) = \tilde{\theta}_{i,j} \quad \text{and} \quad \tilde{\theta}_j(x_{i+1}) = \tilde{\theta}_{i+1,j} \tag{12}$$

has the analytical solution in the interval $[x_i, x_{i+1}]$ as

$$\tilde{\theta}_j(x) = \frac{1}{\sinh\lambda_j\ell}\left[\sinh\lambda_j(x_{i+1} - x)\tilde{\theta}_{i,j} + \sinh\lambda_j(x - x_i)\tilde{\theta}_{i+1,j}\right] \tag{13}$$

Similarly, the analytical solution of Eq. (11) in the interval $[x_{i-1}, x_i]$ is

$$\tilde{\theta}_{j-1}(x) = \frac{1}{\sinh\lambda_{j-1}\ell}\left[\sinh\lambda_{j-1}(x_i - x)\tilde{\theta}_{i-1,j-1} + \sinh\lambda_{j-1}(x - x_{i-1})\tilde{\theta}_{i,j-1}\right] \tag{14}$$

where ℓ denotes the length of sub-space domain or the distance between two neighboring nodes.

In substance, the heat flux and temperature within the whole space domain are continuous, thus the following conditions can be required

$$\tilde{\theta}_{j-1}(x_i) = \tilde{\theta}_j(x_i) \tag{15}$$

and

$$\frac{\mathrm{d}\tilde{\theta}_{j-1}(x_i)}{\mathrm{d}x} = \frac{\mathrm{d}\tilde{\theta}_j(x_i)}{\mathrm{d}x} \tag{16}$$

Substituting Eqs. (13)–(15) into Eq. (16) can produce the following discretized form for the present problem at the ith node as

$$B_{i-1}\tilde{\theta}_{i-1} + B_i\tilde{\theta}_i + B_{i+1}\tilde{\theta}_{i+1} = 0, \quad i = 2, 3, \ldots, m-1 \tag{17}$$

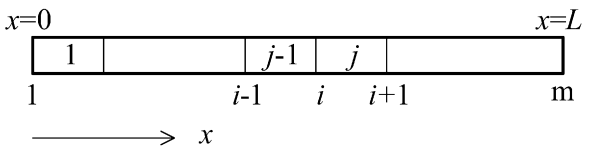

Fig. 1. Geometry and coordinates.

where m is the number of nodes and the coefficients B_{i-1}, B_i, and B_{i+1} are given as

$$B_{i-1} = B_{i+1} = 1.0 \tag{18a}$$

and

$$B_i = -2\cosh\lambda\ell \tag{18b}$$

Rearrangement of Eq. (17) in conjunction with the discretized form of the boundary conditions yields the following matrix equation as

$$[B]\{\tilde{\theta}\} = \{F\} \tag{19}$$

where $[B]$ is a matrix with the complex number s, $\{\tilde{\theta}\}$ is a column vector representing the unknown nodal evaluation temperatures in the Laplace transform domain, and $\{F\}$ is a column vector representing the forcing term. Thereafter, the application of the Gaussian elimination algorithm and the numerical inversion of the Laplace transform [35–38] to Eq. (19) can yield the nodal temperatures in the physical domain.

4. Results and discussion

All present computations are performed for the thermal behaviors in the skin with various surface heatings. Some thermal properties of the sample skin are regarded as $\rho = 1000\ \mathrm{kg/m^3}$ and $C = C_b = 4200\ \mathrm{J/kg\,°C}$ [33]. The distance between the skin and body core and total node number are $L = 0.01208$ m [14] and $m = 151$, respectively. The values of the other parameters are individually determined for each calculation.

4.1. Constant surface temperature heating

For the purpose of comparison, the case illustrated by Liu et al. [33] is first discussed. Liu et al. considered that the skin surface temperature could be kept constant as the skin contacts with a large steel plate at a high temperature. The assumption that heat flux approaches zero deep in tissue $x = L$ was made. The corresponding boundary conditions are considered as [33]

$$\theta(0, t) = \theta_o \quad \text{and} \quad \frac{\partial\theta(L, t)}{\partial x} = 0 \tag{20}$$

and then the Laplace transform of Eq. (20) is

$$\tilde{\theta}(0, s) = \theta_o/s \quad \text{and} \quad \frac{\mathrm{d}\tilde{\theta}(L, s)}{\mathrm{d}x} = 0 \tag{21}$$

where the value of θ_o is specified with 12 °C. Figs. 2–5 plots the calculated results for the case of constant surface temperature heating.

Fig. 2 shows the temperature elevations at $x = 0.00208$ m and $x = 0.01$ m for $W_b = 0.5\ \mathrm{kg/m^3\,s}$, $K = 0.2\ \mathrm{W/m\,°C}$, and $\tau = 0$ and 20 s. The comparison between the present results and the results given by Liu et al. [33] is done. As $\tau = 0$ s, the thermal behavior is described with the Pennes bioheat equation, and thermal signal can reach the specified locations in a very fast velocity and no jump discontinuity happens in the temperature distribution. Due to the effects of relaxation time,

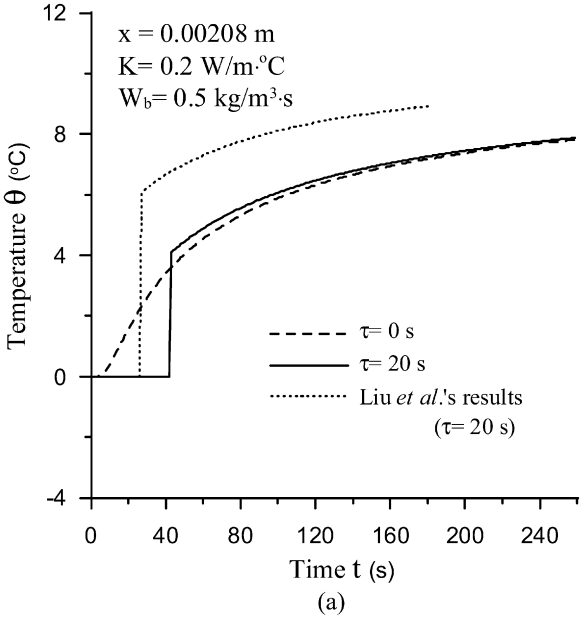

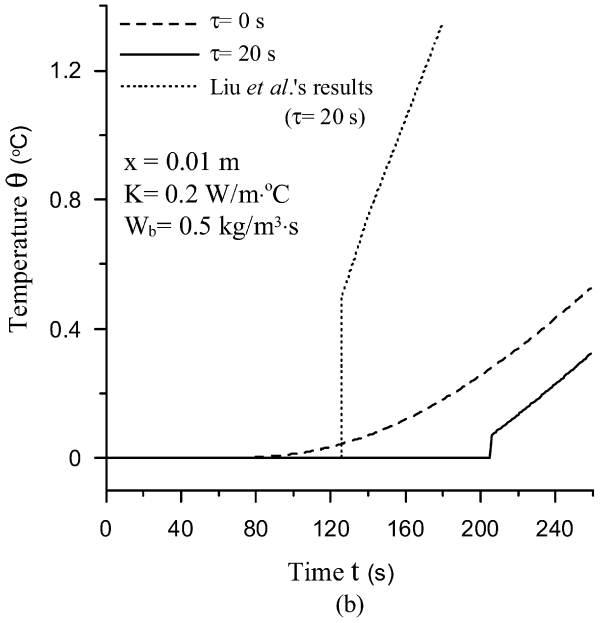

Fig. 2. Thermal response with $K = 0.2\ \mathrm{W/m\,^{\circ}C}$ at (a) $x = 0.00208$ m and (b) $x = 0.01$ m for the case of constant surface temperature heating.

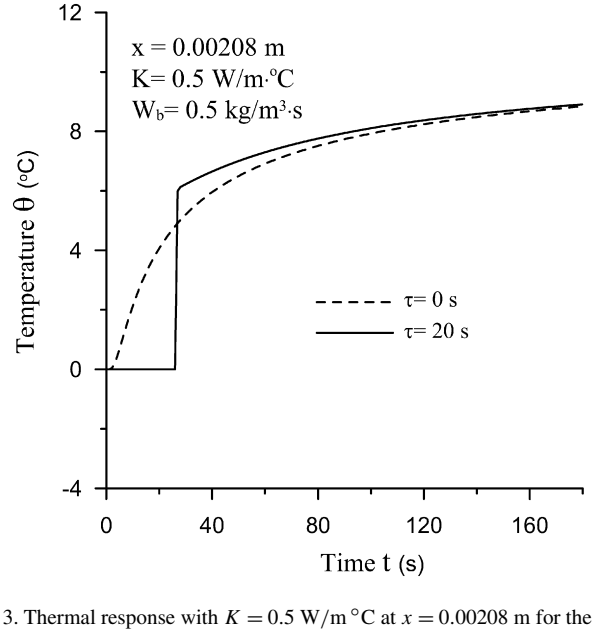

Fig. 3. Thermal response with $K = 0.5\ \mathrm{W/m\,^{\circ}C}$ at $x = 0.00208$ m for the case of constant surface temperature heating.

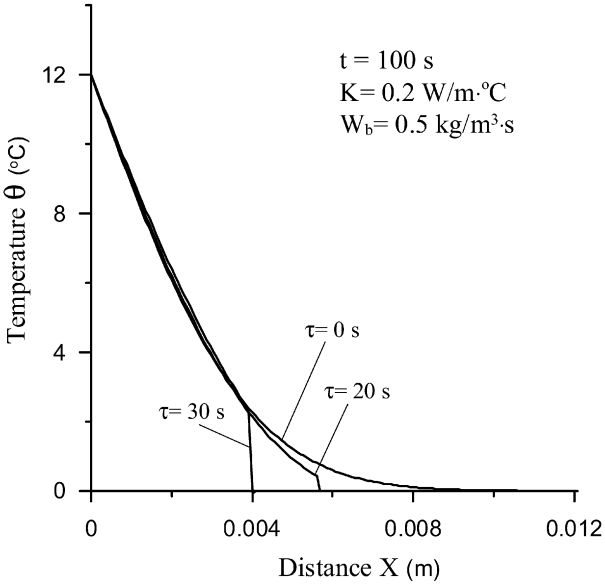

Fig. 4. Effects of relaxation time on the temperature distribution with $K = 0.2\ \mathrm{W/m\,^{\circ}C}$ and $W_b = 0.5\ \mathrm{kg/m^3\,s}$ at $t = 100$ s.

heat propagates in a finite velocity for $\tau = 20$ s. The heat propagation velocity can be obtained from $V = \sqrt{\alpha/\tau}$ [32]. Then, thermal signal can reach the location $x = 0.00208$ m at $t = 0.00208/V = 0.00208/\sqrt{0.2/(1000 \times 4200 \times 20)} = 42.627$ (s) and can reach the location $x = 0.01$ m at $t = 0.01/V = 0.01/\sqrt{0.2/(1000 \times 4200 \times 20)} = 204.939$ (s). This phenomenon is found in Fig. 2. The transient temperature at $x = 0.01$ m for $\tau = 0$ s are higher than that for $\tau = 20$ s due to the effects of finite heat propagation. However, the present results do not agree with the results given by Liu et al. [33].

In order to further test the accuracy of the present numerical scheme, Fig. 3 plots the thermal response at $x = 0.00208$ m computed with $W_b = 0.5\ \mathrm{kg/m^3\,s}$, $K = 0.5\ \mathrm{W/m\,^{\circ}C}$, and $\tau = 0$ and 20 s. The computed results are the same with those given by Liu et al. [33]. The thermal signal has reached $x = 0.00208$ m at $t = 0.00208/\sqrt{0.5/(1000 \times 4200 \times 20)} = 26.96$ (s). This implies that the present numerical scheme is efficient and accurate for such problems. This phenomenon and the results in Fig. 2 show that there may be a wrong typewriting for the value of K in the literature [33]. In other words, $K = 0.2\ \mathrm{W/m\,^{\circ}C}$ specified in the literature [33] may need to be corrected with $K = 0.5\ \mathrm{W/m\,^{\circ}C}$.

Fig. 4 demonstrates the effects of relaxation time on the temperature distribution with $K = 0.2\ \mathrm{W/m\,^{\circ}C}$ and $W_b = 0.5\ \mathrm{kg/m^3\,s}$ at $t = 100$ s. As $\tau \neq 0$, the heat transfer has a phenomenon of wave-like propagation which will dissipate with

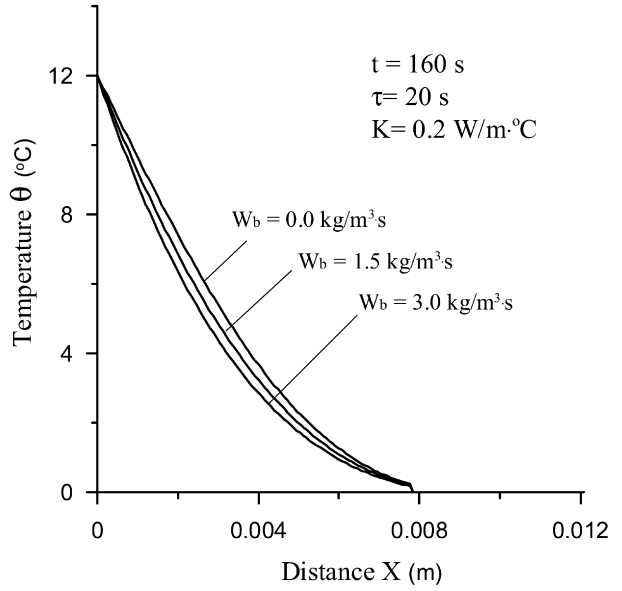

Fig. 5. Temperature distributions with $K = 0.2\ \mathrm{W/m\,^{\circ}C}$ and $\tau = 20$ s at $t = 160$ s for various W_b values.

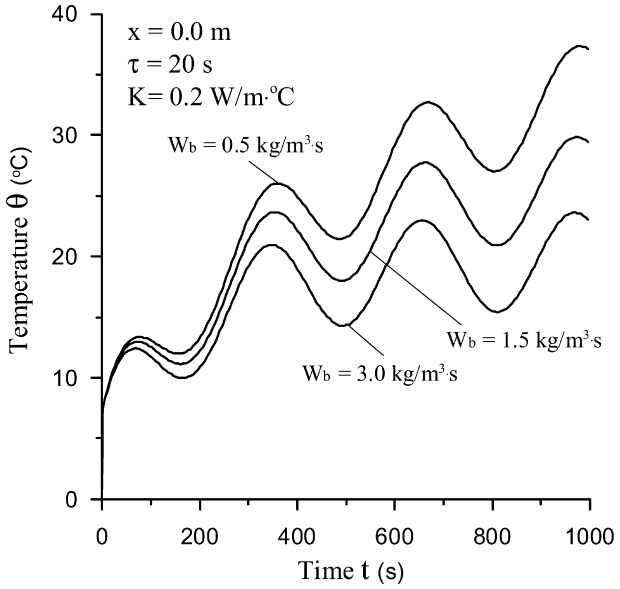

Fig. 6. Effects of the blood perfusion rate W_b on the variation of the temperature θ at $x = 0$ with $K = 0.2\ \mathrm{W/m\,^{\circ}C}$ and $\tau = 20$ s.

time. The thermal wave propagation is dominant when τ is large. The penetration depth of the thermal signal for $\tau \neq 0$ is equal to the computed value $x = V \times t$ and is inversely proportional to the value of τ. As $\tau = 0$ s, the thermal behavior in living tissue undergoes to the traditional bioheat transfer and the temperatures in the area $x > 0.01$ m approach to zero for retention of energy.

The perfusion rate of blood plays an important role in bioheat transfer. The discussion about the effects of the perfusion rate of blood on the temperature distribution is needed. Fig. 5 shows the temperature distributions with $K = 0.2\ \mathrm{W/m\,^{\circ}C}$ and $\tau = 20$ s at $t = 160$ s for various W_b values. The blood perfusion develops a cooling function, since the skin temperature is higher than the arterial temperature. The heat energy taken away by the blood is proportional to the perfusion rate. Thus, it is found from Fig. 5 that the skin temperature for $W_b = 3.0\ \mathrm{kg/m^3\,s}$ is lower than that for $W_b = 1.5\ \mathrm{kg/m^3\,s}$ and $W_b = 0\ \mathrm{kg/m^3\,s}$. It is also observed that the thermal wave fronts locate at the same position.

4.2. Sinusoidal surface heating

The repeated irradiation from regulated laser can cause this kind of heating. It was used to estimate the blood perfusion [12]. Under the consideration that the biological body tends to maintain the core temperature constant, the core temperature was frequently regarded as the steady-state temperature [2–4]. As a result, the boundary conditions for this case are described as

$$q(0,t) = q_0 + q_w \cos(wt) \tag{22}$$

$$\theta(L,t) = 0 \tag{23}$$

where q_0 and q_w are the constant term and the amplitude of sinusoidal surface heating. This work computes the results induced with the surface heating $q(0,t) = 1000 + 500\cos(0.02t)$.

Fig. 6 demonstrates the effects of the blood perfusion rate W_b on the variation of the temperature θ at $x = 0$ with $K = 0.2\ \mathrm{W/m\,^{\circ}C}$ and $\tau = 20$ s. During $0 < t < 0.01028/\sqrt{0.2/(1000 \times 4200 \times 20)} = 210.677$ (s), the thermal signal has not reached the boundary surface $x = L$, and no heat flux loses from the boundary surfaces. At the same time, the difference between the surface temperature and the arterial temperature is small at the initial times, and the heat energy carried off by the perfusion blood is not much. Therefore, the temperature obviously increases as shown in Fig. 6. After that, the rising rate of the surface temperature is slowed down for the cooling function of the blood perfusion. Also, the larger the blood perfusion rate, the shorter time to prevent the surface temperature rising.

The heat propagation velocity is proportional to the thermal diffusivity α and is inversely proportional to the relaxation time τ for the definition of the heat propagation velocity $V = \sqrt{\alpha/\tau}$ [32]. It is well known that the thermal diffusivity α is defined by $K/\rho C$. The heat propagation velocity is also proportional to the conductivity K. Fig. 7 plots the temperature distributions with $W_b = 0.5\ \mathrm{kg/m^3\,s}$ and $\tau = 20$ s for various K values at $t = 200$ s. It is found from this figure that the temperature distribution curve for $K = 1.0\ \mathrm{W/m\,^{\circ}C}$ is smoother. That is, the heat propagation velocity is raised by the larger K value, and energy heating on the boundary surface $x = 0$ transfers through the sample skin in conduction behavior in a shorter time period. The oscillation phenomenon caused by sinusoidal surface heating is decayed in the inner.

4.3. Step surface heating

Skin burns due to a flash fire, hot plate, liquid, and gas for a short period of time belong to such problem [3,14]. The boundary conditions for this case are written as

$$q(0,t) = q_0\big[u(t) - u(t-a)\big] \tag{24}$$

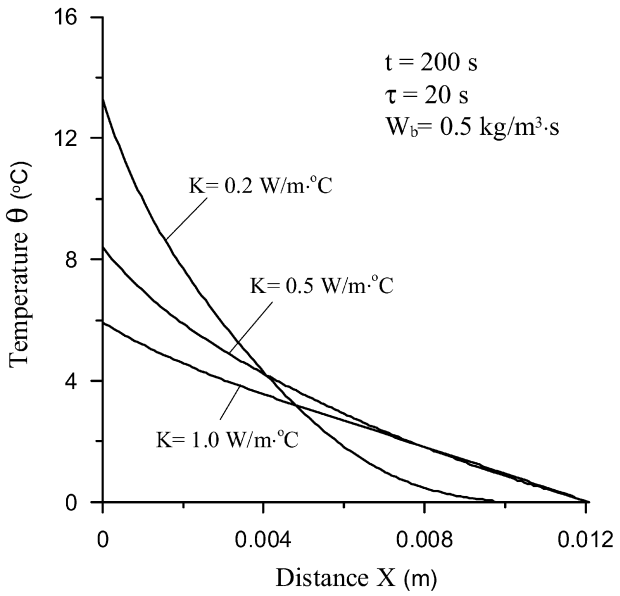

Fig. 7. Temperature distributions with $W_b = 0.5\ \mathrm{kg/m^3\,s}$ and $\tau = 20$ s for various K values at $t = 200$ s.

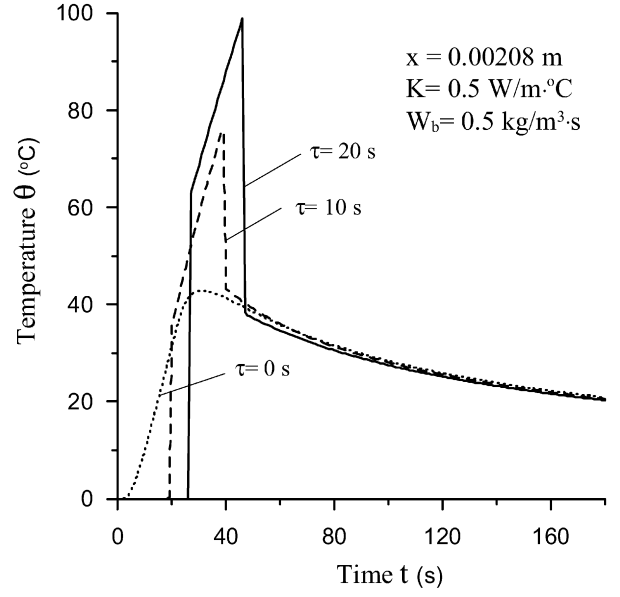

Fig. 8. Effects of the relaxation time τ on the temperature response at $x = 0.00208$ m for $K = 0.5\ \mathrm{W/m\,°C}$ and $W_b = 0.5\ \mathrm{kg/m^3\,s}$.

$$\theta(L,t) = 0 \tag{25}$$

The function $u(t)$ in Eq. (24) is step function. The computations of this case are performed with $q_0 = 40000\ \mathrm{W/m^2}$ and $a = 20$ s.

Fig. 8 shows the effects of the relaxation time τ on the temperature response at $x = 0.00208$ m for $K = 0.5\ \mathrm{W/m\,°C}$ and $W_b = 0.5\ \mathrm{kg/m^3\,s}$. The time that the thermal signal for $\tau = 20$ s reaches the location $x = 0.00208$ m is longer than those for $\tau = 0$ s and $\tau = 10$ s, because the heat propagation velocity is inversely proportional to the relaxation time τ. As $\tau = 0$ s, the shape structure of thermal pulse is decayed due to fading of thermal wave effects. For the effects of the relaxation time,

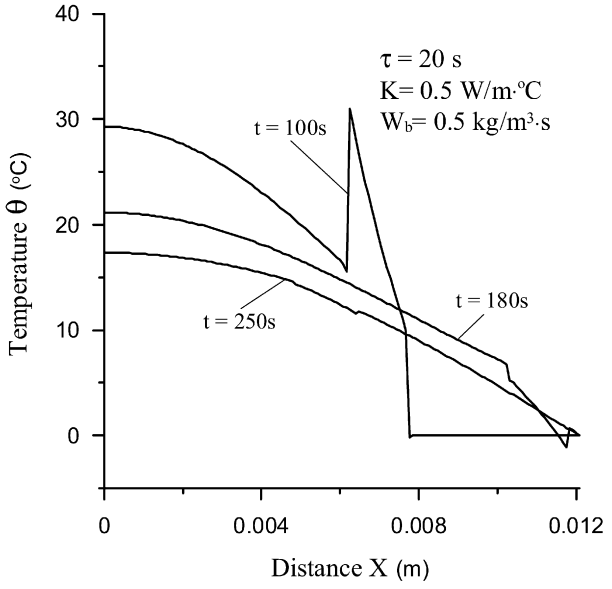

Fig. 9. Temperature distributions with $\tau = 20$ s, $K = 0.5\ \mathrm{W/m\,°C}$, and $W_b = 0.5\ \mathrm{kg/m^3\,s}$ at various times.

the temperature response is higher at $\tau = 20$ s. The shape structure of thermal pulse is kept for $\tau = 10$ s and $\tau = 20$ s, while it fades away for $\tau = 0$ s. Honner [39] stated that it is hard to dampen the numerical oscillations of a problem with two wave fronts caused by the pulsed surface heat flux. However, no numerical oscillation is found in the present results. Obviously, the present numerical scheme can accurately obtain the numerical results of such a problem.

Fig. 9 plots the temperature distributions with $\tau = 20$ s, $K = 0.5\ \mathrm{W/m\,°C}$, and $W_b = 0.5\ \mathrm{kg/m^3\,s}$ at various times. As $t = 100$ s, thermal signal has not reached the boundary surface $x = L$, and the temperature distribution is not affected by the boundary condition at $x = L$. Due to sudden heating, the thermal wave effect dominates the behavior of heat transfer [32]. It is easy to create high temperature and may have burn injury around the thermal pulse. At $t = 180$ s, the thermal pulse has encountered the boundary surface $x = L$, and a downward reflected thermal wave is induced for the boundary condition (25). The downward reflected thermal wave makes the tissue temperature below to the initial temperature. This is a physically doubtful result, but it is admitted for the wave propagation concept. Taitel [40] had discussed the thermodynamic validity of the hyperbolic heat conduction equation for the above phenomenon by suggesting a different conduction equation based on the 'random walk' process. Barletta and Zanchini [41] on the other hand reported that if the decay of the boundary heat flux is not steeper than the function $\exp(-t/\tau)$, the wave-like thermal behavior is compatible with the local equilibrium scheme. In this case, the decay of the boundary heat flux is steeper than the function $\exp(-t/\tau)$ at $t = 20$ s. Whether this physically doubtful solution is accurate can only be shown through further experiments. As $t = 250$ s, the tissue has been cooled for the cooling function of blood perfusion and the effect of the boundary condition at $x = L$.

5. Conclusions

The behaviors of finite heat propagation in a sample skin subjected to constant, sinusoidal, or step surface heatings, which are caused from repeated and regulated laser irradiation for estimating the blood perfusion or skin burns for a short period of time, are analyzed with the thermal wave model of bioheat transfer. Due to the effects of finite heat propagation and the discontinuous time-dependent surface heat flux, constant and step surface heatings induce the discontinuous temperature distributions. The suppression of numerical oscillations in the vicinity of sharp discontinuities is the major difficulty for numerically solving such problems. This paper develops a modified discretization scheme based on the Laplace transform to solve the present problem, and the present numerical results do not exhibit severe numerical oscillations in the vicinity of the jump discontinuity. The downward reflected thermal wave, which is created at the boundary end kept at the initial temperature, can make the transient tissue temperature below to the initial temperature. The blood perfusion develops the cooling function to prevent the tissue temperature rising, but does not affect the thermal propagation velocity.

References

[1] H. Arkin, L.X. Xu, K.R. Holmes, Recent developments in modeling heat transfer in blood perfused tissues, IEEE Trans. Biomed. Engrg. 41 (1994) 97–107.

[2] D.A. Nelson, M.T. Nelson, T.J. Walters, P.A. Mason, Skin heating effects of millimeter-wave irradiation—thermal modeling results, IEEE Trans. Microwave Theory Techniques 48 (2000) 2111–2120.

[3] Z.S. Deng, J. Liu, Analytical study on bioheat transfer problems with spatial or transient heating on skin surface or inside biological bodies, J. Biomed. Engrg. 124 (2002) 638–649.

[4] L. Hu, A. Gupta, J.P. Gore, L.X. Xu, Effect of forced convection on the skin thermal expression of breast cancer, J. Biomed. Engrg. 126 (2004) 204–211.

[5] Y. Rabin, A. Shitzer, Numerical solution of the multidimensional freezing problem during cryosurgery, J. Biomed. Engrg. 120 (1998) 32–37.

[6] J. Zhang, G.A. Sandison, J.Y. Murthy, L.X. Xu, Numerical simulation for heat transfer in prostate cancer cryosurgery, J. Biomed. Engrg. 127 (2005) 279–294.

[7] J. Liu, L.X. Xu, Boundary information based diagnostics on the thermal states of biological bodies, Int. J. Heat Mass Transfer 43 (2000) 2827–2839.

[8] E. Aren, P. Bosselmann, Wind, sun and temperature predicting the thermal comfort of people in outdoor spaces, Building Environ. 24 (1989) 315–320.

[9] J.C. Chato, Measurement of thermal properties of growing tumors, Ann. N.Y. Acad. Sci. 355 (1980) 67–85.

[10] M.M. Chen, K.R. Holmes, V. Rupinskas, Pulse-decay method for measuring the thermal conductivity of living tissues, J. Biomed. Engrg. 103 (1981) 253–260.

[11] J.W. Valvano, J.T. Allen, H.F. Bowman, The simultaneous measurement of thermal conductivity, thermal diffusivity, and perfusion in small volumes of tissue, J. Biomed. Engrg. 106 (1984) 192–197.

[12] J. Liu, L.X. Xu, Estimation of blood perfusion using phase shift in temperature response to sinusoidal heating at the skin surface, IEEE Trans. Microwave Theory Techniques 46 (1999) 1037–1043.

[13] K.R. Diller, Modeling of bioheat transfer processes at high and low temperatures, Adv. Heat Transfer 22 (1992) 157–357.

[14] D.A. Torvi, J.D. Dale, A finite element model of skin subjected to a flash fire, J. Biomed. Engrg. 116 (1994) 250–255.

[15] E.Y.K. Ng, L.T. Chua, Mesh independent prediction of skin burns injury, International J. Med. Engrg. Technol. 24 (2000) 255–261.

[16] E.Y.K. Ng, L.T. Chua, Comparison of one- and two-dimensional programmes for predicting the state of skin burns, Burns 28 (2002) 27–34.

[17] E.Y.K. Ng, L.T. Chua, Quick numerical assessment of skin burn injury with spreadsheet in PC, J. Mech. Med. Biol. 1 (2001) 1–10.

[18] E.Y.K. Ng, L.T. Chua, Parametric and sensitivity analysis on prediction of skin burn injury, in: Proc. IMechE, Part H, Int. J. Engrg. Med. 216 (2002) 157–170.

[19] S.C. Jiang, N. Ma, H.J. Li, X.X. Zhang, Effects of thermal properties and geometrical dimensions on skin burn injuries, Burns 28 (2002) 713–717.

[20] C. Cattaneo, Sulla conduzione de calore, Atti del Semin. Mat. E Fis. Univ. Modena 3 (1948) 83–101.

[21] P. Vernotte, Les paradoxes de la théorie continue de l'équation de la chaleur, Compte Rendus 246 (1958) 3145–3155.

[22] H.D. Weymann, Finite speed of propagation in heat conduction, diffusion, and viscous shear motion, Amer. J. Phys. 35 (1967) 488–496.

[23] S.L. Sobolev, Transport processes and traveling waves in systems with local nonequilibrium, Sov. Phys. Usp. 34 (1991) 217–229.

[24] M.N. Özisik, D.Y. Tzou, On the wave theory in heat conduction, ASME J. Heat Transfer 116 (1994) 526–535.

[25] A.V. Luikov, Analytical Heat Diffusion Theory, Academic Press, New York, 1968, pp. 245–248.

[26] W. Kaminski, Hyperbolic heat conduction equation for material with a nonhomogenous inner structure, ASME J. Heat Transfer 112 (1990) 555–560.

[27] A.M. Braznikov, V.A. Karpychev, A.V. Luikova, One engineering method of calculating heat conduction process, Inzhenerno Fiz. Zh. 28 (1975) 677–680.

[28] K. Mitra, S. Kumar, A. Vedavarz, M.K. Moallemi, Experimental evidence of hyperbolic heat conduction in processed meat, ASME J. Heat Transfer 117 (1995) 568–573.

[29] W. Roetzel, N. Putra, S.K. Das, Experiment and analysis for non-Fourier conduction in materials with non-homogeneous inner structure, Int. J. Thermal Sci. 42 (2003) 541–552.

[30] A. Graßmann, F. Peters, Experimental investigation of heat conduction in wet sand, Heat Mass Transfer 35 (1999) 289–294.

[31] H. Herwing, K. Beckers, Experimental evidence about the controversy concerning Fourier or non-Fourier heat conduction in materials with a non-homogeneous inner structure, Heat Mass Transfer 36 (2000) 387–392.

[32] W.H. Yang, Thermal (heat) shock biothermomechanical viewpoint, J. Biomed. Engrg. 115 (1993) 617–621.

[33] J. Liu, X. Chen, L.X. Xu, New thermal wave aspects on burn evaluation of skin subjected to instantaneous heating, IEEE Trans. Biomed. Engrg. 46 (1999) 420–428.

[34] W.Q. Lu, J. Liu, Y. Zeng, Simulation of the thermal wave propagation in biological tissues by the dual reciprocity boundary element method, Engrg. Anal. Boundary Elements 22 (1998) 167–174.

[35] K.C. Liu, Analysis of dual-phase-lag thermal behavior in layered films with temperature-dependent interface thermal resistance, J. Phys. D: Appl. Phys. 38 (2005) 3722–3732.

[36] K.C. Liu, P.J. Cheng, Numerical analysis for dual-phase-lag heat conduction in layered films, Numer. Heat Transfer, Part A 49 (2006) 589–606.

[37] K.C. Liu, Numerical simulation for non-linear thermal wave, Appl. Math. Comput. 175 (2006) 1385–1399.

[38] K.C. Liu, Analysis for microscopic hyperbolic two-step heat transfer problems, Int. J. Thermophys. 27 (2006) 596–613.

[39] M. Honner, Heat waves simulation, Comput. Math. Appl. 38 (1999) 233–243.

[40] Y. Taitel, On the parabolic, hyperbolic and discrete formulation of the heat conduction equation, Int. J. Heat Mass Transfer 15 (1971) 369–371.

[41] A. Barletta, E. Zanchini, Hyperbolic heat conduction and local equilibrium: a second law analysis, I, J. Heat and Mass Transfer 40 (1997) 1007–1016.